International Journal of Control and Automation
Vol. 10, No. 2 (2017), pp.213-228
http//dx.doi.org/10.14257/ijca.2017.10.2.18

Single Phase Current Sensor-Based Model Predictive Torque Control for PMSM Drives

Qingfang Teng[1], Shuyuan Li[2] and Jianyong Bai[1]

[1]*Department of Automation and Electrical Engineering, Lanzhou Jiaotong University, Lanzhou, Gansu 730070, PRC*
[2]*Graduate Management Team, Engineering University of the Armed Police Force, Xi'an, Shan'xi 710086, PRC*
tengqf@mail.lzjtu.cn, 379467329@qq.com, bai jian yong@163.com

Abstract

A novel adaptive observer for estimating stator currents and resistance is proposed for three-phase permanent magnet synchronous motor (PMSM) drives. It is used to formulate single-phase-current-sensor-based model predictive torque control (MPTC) drives. Generally two phase-current sensors are indispensable for feedback control in PMSM drives. Nevertheless, failure of one phase-current sensor could results in performance degradation of PMSM drives if it is not compensated. Furthermore, PMSM drives are required to be robust to stator resistance variation. The proposed adaptive observer is capable of estimating stator currents with online tuning of stator resistance while rotor speed & position and only one phase current are available. Stability of the observer is analytically verified based on Lyapunov stability theory. In order to reduce torque and flux ripples and improve drives control performance, MPTC strategy is employed. The proposed MPTC scheme incorporating the adaptive observer can ensure that the whole PMSM drives achieve satisfactory torque & speed control performance and improve strong robustness. And the designed system can be used for the purpose of phase current sensor fault tolerant and then cost reduction. Comprehensive simulation validates the feasibility and effectiveness of the proposed scheme.

Keywords*: Model predictive torque control, Permanent magnet synchronous motor, Current sensorless, Adaptive observer*

1. Introduction

Permanent magnet synchronous motor (PMSM) drives are nowadays widely used in the industry applications due to its capability of field-weakening control, its high efficiency and high power/torque density. For PMSM drives, instantaneous stator currents are required for successful operation of the feedback control. As a result, two phase current sensors are installed in conventional three-phase voltage-source inverters (VSI). Nevertheless, sudden severe failure of phase current sensors would result in the over-current malfunction of the system. And if there is no protection scheme in the gate-drive circuit, the failure would lead to irrecoverable fault of power semiconductors in VSI, which causes degradation of motor drive performance. Additionally, the minor failures (such as gain drift and nonzero offset) of phase current sensors would result in torque pulsation synchronizing with the inverter output frequency [1]. The larger offset and scaling error of phase current sensors would bring about the worse performance of torque regulation. Moreover, if the offset and gain drift are above some certain level, it would cause over-current trip at high speed and in heavy load conditions [2]. So it is necessary to consider fault-tolerant operation of phase current sensors.

ISSN: 2005-4297 IJCA

The current sensorless technology, regarded as fault-tolerant one, has been developed in the past few decades, which replaces physical fault current sensor with virtual sensor (or current estimator). This technology has several advantages such as high reliability and low cost. Moreover, it allows motor to work in hostile environment and occupy small available space owing to omitting physical current sensor.

As far as the current sensorless technique is concerned, several estimation methods have been reported. The mainstream proposed first by J.T.Boys [3] concentrates on estimating phase currents from DC-link current sensor in VSI, which needs the information of the switching states in VSI. The drawback of the technique is that on one hand, the duration of an active switching state may be so short that the DC-link current cannot be measured. On the other hand, there are immeasurable regions in the output voltage hexagon where the current sampling and reconstruction is limited or impossible to do [4]. In addition, the DC-link sensed current remains sensitive to the narrow pulse and further deteriorates if the cable capacitance causes spurious oscillations in the DC-link waveform. In order to provide high-accuracy phase current reconstruction over a wide range of operating conditions with a low current waveform, over the past years, many kinds of methods of improved PWM modulation strategy have been proposed for the single DC-link current sensor technique [5]-[16]. Although many improvement methods show reasonable phase current reconstruction performance, these methods suffer from complicated algorithms to implement phase current estimation [17]. Except the aforementioned mainstream, there have appeared other current estimation methods in recent years [18] and [19]. Reference [18] introduced phase current estimation by using the synchronous reference frame variables for induction motor (IM) drive. Though this algorithm was simple, it did not show how to extract the reference *d*-axis current involved. In [19], current & position estimator was designed based on the search coil model for PMSM drives. The technique developed a backup universal sensor concept, but extra search coil in demand boosted cost and hardware complexity.

In recent two or three years, a new adaptive observer-based reconstruction of phase currents was put forward in the literatures [20] and [21]. Employing this technique, [20] reconfigured phase currents for IM drive using single phase current sensor, while [21] reconfigured phase currents for PMSM drives without any phase current sensor. Still, taking the problem of stator resistance adjustment into account, so far there is no report on estimation of unmeasured phase currents when only one phase-current is available for PMSM drives.

For PMSM drives, popular drive control strategies include two types: field oriented control strategy (FOC) and direct torque control (DTC). Due to the inherent bandwidth of inner current loop, the dynamic response of FOC drive systems is limited. To improve the dynamic performance, DTC has recently begun to be applied [22]. Compared to FOC, DTC directly manipulates the inverter's output voltage vector and hence eliminates the inherent delay caused by current loops and features comparatively good dynamic response. Even so, switching-table-based DTC presents some unavoidable drawbacks, such as high torque and flux ripples, variable switching frequency along with acoustic noise.

Apart from FOC and DTC, model predictive torque control (MPTC) is an emerging control concept and is received significant attention from electrical drives community [23]-[33] which adopts the principle of model predictive control (MPC) [34]. MPC has several merits such as easy inclusion of nonlinearities and constraints. Besides, its algorithm is simple and then its implementation is easy. Compared with previous two state-of-the art schemes, MPTC achieves more obvious reduction of the torque and flux ripples [35]. Furthermore, switching losses can be

reduced [36]. Even so, MPTC has not yet been applied to current sensorless PMSM drive system.

In this paper, for PMSM drives with single phase current sensor, a novel adaptive observer-based MPTC drive system is designed. Taking stator resistance variation into account, the proposed observer is capable of estimating stator currents with online tuning of stator resistance based on measurement of rotor speed and position. The proposed single-phase-current-sensor-based MPTC can improve PMSM drives' performance and robustness.

The structure of the paper is as follows: modeling of PMSM is given in Section two. In Section three, MPTC system with an adaptive observer is constructed, and then adaptive observer and MPTC are designed, respectively. The numerical simulation results & analysis and conclusion are reported in Section four and five, respectively.

2. Dynamic Model of PMSM

As for three-phase PMSM, the models in rotor synchronous reference frame (*dq*-frame) and two-phase stationary reference frame (*αβ*-frame) are expressed as follows, respectively,

$$\begin{cases} \dfrac{\mathrm{d}i_d}{\mathrm{d}t} = \dfrac{1}{L_d}(u_d - R_s i_d + \mathrm{p}\omega_r L_q i_q) \\ \dfrac{\mathrm{d}i_q}{\mathrm{d}t} = \dfrac{1}{L_q}(u_q - R_s i_q - \mathrm{p}\omega_r (L_d i_d + \psi_m)) \end{cases} \tag{1}$$

$$\begin{cases} \dfrac{\mathrm{d}i_\alpha}{\mathrm{d}t} = \dfrac{1}{L_\alpha}(u_\alpha - R_s i_\alpha + \mathrm{p}\omega_r \psi_m \sin\theta) \\ \dfrac{\mathrm{d}i_\beta}{\mathrm{d}t} = \dfrac{1}{L_\beta}(u_\beta - R_s i_\beta - \mathrm{p}\omega_r \psi_m \cos\theta) \end{cases} \tag{2}$$

where

R_s	resistance of the stator windings
L_d, L_q	*dq*-axes stator inductances
L_α, L_β	*αβ*-axes stator inductances
ψ_m	permanent magnet flux
u_d, u_q	*dq*-axes stator voltages
u_α, u_β	*αβ*-axes stator voltages
i_d, i_q	*dq*-axes stator currents
i_α, i_β	*αβ*-axes stator currents
ω_r	mechanical rotor speed
p	number of pole pairs
θ	rotor electrical position

And mechanical equation is expressed as

$$\frac{\mathrm{d}\omega_r}{\mathrm{d}t} = \frac{1}{J}\left(T_e - T_l - B_m\omega_r - T_f\right) \tag{3}$$

where

J	inertia of moment
T_l	load torque
B_m	viscous friction coefficient
T_f	coulomb friction torque
T_e	electromagnetic torque, it can be expressed as

$$T_e = \frac{3p}{2}\left[\psi_m i_q + \left(L_d - L_q\right) i_d i_q\right] \tag{4}$$

3. Design of MPTC System Using an Adaptive Observer

The objective of MPTC system based on an adaptive observer is that the PMSM drive system can work reliably and its speed and torque can be controlled not only to have satisfactory performance but also to be strong robust to stator resistance variation and external disturbance. The schematic of MPTC system based on an adaptive observer is shown in Figure 1.

MPTC drive system mainly comprises of five components: adaptive observer, MPTC, Maximum Torque per Ampere (MTPA) (used for calculating reference stator flux linkage), Power unit and PI controller, respectively.

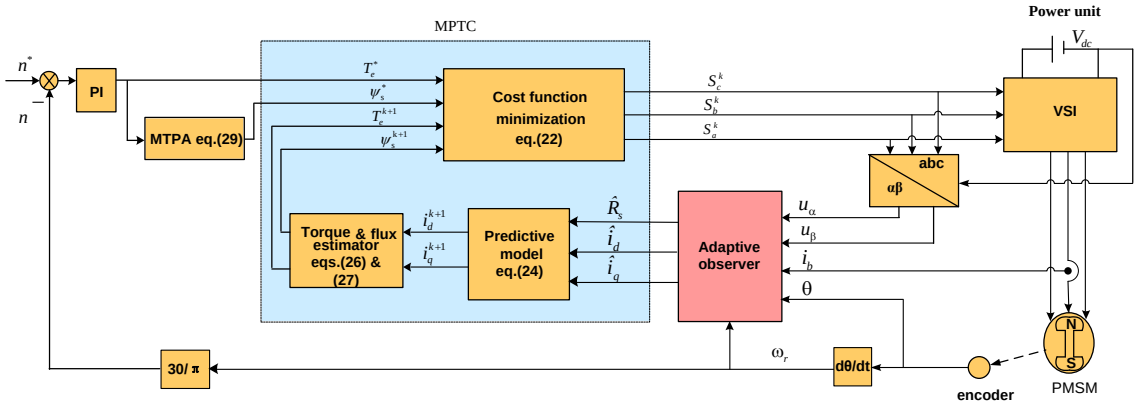

Figure 1. Block Diagram of MPTC System Based on Adaptive Observer

3.1. Adaptive Observer Design

In this section, a novel adaptive observer is designed to estimate stator currents and stator resistance when failure of one phase current sensor happens. In the observer design process, the following practical assumption is considered:

1) Only one phase current sensor is used. Here, we assume that only phase-*b* is measured and the other currents sensors are not available.

2) Inverter input voltage, rotor speed and position can be measured.

3) Due to heating during operating of the motor, the stator resistance R_s is considered as uncertain parameter while other motor parameters are measured offline and constant during the motor operation.

4) There is no saturation in the magnetic circuit.

For surface-mounted PMSM, $L_d = L_q = L_\alpha = L_\beta = L$. The α-axis in $\alpha\beta$-frame is oriented along phase-*a* axis in three-phase stationary reference frame (*abc*-frame). The *abc*-axes stator currents in *abc*-frame have relationship with $\alpha\beta$-axes ones in $\alpha\beta$-frame using the following transformation matrix:

$$\begin{bmatrix} i_a \\ i_b \\ i_c \end{bmatrix} = \begin{bmatrix} 1 & 0 \\ -1/2 & \sqrt{3}/2 \\ -1/2 & -\sqrt{3}/2 \end{bmatrix} \begin{bmatrix} i_\alpha \\ i_\beta \end{bmatrix} \tag{5}$$

where i_a, i_b and i_c are *abc*-axes stator currents in *abc*-frame.

From (5), it follows that

$$i_b = -\frac{1}{2} i_\alpha + \frac{\sqrt{3}}{2} i_\beta \tag{6}$$

Taking (2) into account, the time derivative of (6) is determined to be

$$\begin{aligned} \frac{\mathrm{d}i_b}{\mathrm{d}t} &= \frac{\sqrt{3}}{2L}[u_\beta - R_s(\frac{1}{\sqrt{3}} i_\alpha + \frac{2}{\sqrt{3}} i_b) - \mathrm{p}\omega_r \psi_\mathrm{m} \cos\theta] - \frac{1}{2L}(u_\alpha - R_s i_\alpha + \mathrm{p}\omega_r \psi_\mathrm{m} \sin\theta) \\ &= \frac{\sqrt{3}u_\beta - u_\alpha - 2R_s i_b - \mathrm{p}\omega_r \psi_\mathrm{m}(\sqrt{3}\cos\theta + \sin\theta)}{2L} \end{aligned} \tag{7}$$

The following observer is proposed in order to estimate phase-*b* current,

$$\begin{aligned} \frac{\mathrm{d}\hat{i}_b}{\mathrm{d}t} &= \frac{\sqrt{3}}{2L}[u_\beta - \hat{R}_s(\frac{1}{\sqrt{3}} \hat{i}_\alpha + \frac{2}{\sqrt{3}} i_b) - \mathrm{p}\omega_r \psi_\mathrm{m} \cos\theta] - \frac{1}{2L}(u_\alpha - \hat{R}_s \hat{i}_\alpha + \mathrm{p}\omega_r \psi_\mathrm{m} \sin\theta) - k_1 f(\tilde{i}_b) - k_2 \tilde{i}_b \\ &= \frac{1}{2L}[\sqrt{3}u_\beta - u_\alpha - 2\hat{R}_s i_b - \mathrm{p}\omega_r \psi_\mathrm{m}(\sqrt{3}\cos\theta + \sin\theta)] - k_1 f(\tilde{i}_b) - k_2 \tilde{i}_b \end{aligned} \tag{8}$$

where sign "$\wedge$" denotes the estimated states or parameters. $k_1 f(\tilde{i}_b)$ and $k_2 \tilde{i}_b$ are correctors, k_1 and k_2 are the positive observer gains, and $f(.)$ denotes nonlinear function of phase-*b* current estimation error $\tilde{i}_b$, which is defined,

$$\tilde{i}_b = \hat{i}_b - i_b \tag{9}$$

Definite the following stator resistance estimation error,

$$\tilde{R}_s = \hat{R}_s - R_s \tag{10}$$

The dynamics of the phase-*b* current estimation error, obtained by subtracting (8) from (7), is given by

$$\frac{\mathrm{d}\tilde{i}_b}{\mathrm{d}t} = -\frac{1}{L} \tilde{R}_s i_b - k_1 f(\tilde{i}_b) - k_2 \tilde{i}_b \tag{11}$$

In order to determine the adaptive law for stator resistance and choose observer gains, the following candidate Lyapunov function is selected:

$$V = \frac{1}{2}(\tilde{i}_b^2 + \frac{1}{r} \tilde{R}_s^2) \tag{12}$$

where r is constant positive scalar.

The time derivative of (12) is determined to be

$$\frac{\mathrm{d}V}{\mathrm{d}t} = -k_2 \tilde{i}_b^2 - k_1 f(\tilde{i}_b) \tilde{i}_b + \tilde{R}_s(\frac{1}{r} \frac{d\tilde{R}_s}{dt} - \frac{1}{L} i_b \tilde{i}_b) \tag{13}$$

If we choose following equality,

$$\frac{1}{r} \frac{\mathrm{d}\tilde{R}_s}{\mathrm{d}t} - \frac{1}{L} i_b \tilde{i}_b = 0 \tag{14}$$

then (13) can be rewritten as below

$$\frac{\mathrm{d}V}{\mathrm{d}t} = -k_2 \tilde{i}_b^2 - k_1 f(\tilde{i}_b) \tilde{i}_b \tag{15}$$

To render $\dot{V}$ negative, we suppose

$$f(\tilde{i}_b) = \mathrm{sign}(\tilde{i}_b) \tag{16}$$

then we have

$$\frac{\mathrm{d}V}{\mathrm{d}t} < 0$$

As a result, by Lyapunov stability theorem, dynamics system (11) is stable, which guarantees that both $\tilde{i}_b$ and $\tilde{R}_s$ converge to zero. Since the variation of the stator resistance in the observer time scale is negligible, *i.e.*, $\dot{R}_s \approx 0$, then we have

$$\frac{\mathrm{d}\tilde{R}_s}{\mathrm{d}t}=\frac{\mathrm{d}\hat{R}_s}{\mathrm{d}t}-\frac{\mathrm{d}R_s}{\mathrm{d}t}\approx\frac{\mathrm{d}\hat{R}_s}{\mathrm{d}t} \tag{17}$$

Thus from (14), the adaptive mechanism of stator resistance is derived as follows:

$$\hat{R}_s=\frac{r}{L}\int(i_b\tilde{i}_b)\mathrm{d}t \tag{18}$$

With the adaptive mechanism in (18), estimation value of the stator resistance converges to its real value.

In order to improve the accuracy of the stator resistance estimation and ensure a null steady error, on the base of PI strategy, (18) is modified as below,

$$\hat{R}_s=\frac{r}{L}\{K_{P(R_s)}[i_b(\hat{i}_b-i_b)]+K_{I(R_s)}\int[i_b(\hat{i}_b-i_b)]\mathrm{d}t\} \tag{19}$$

where $K_{P(R_s)}$ and $K_{I(R_s)}$ are proportional and integral scalars, respectively.

By replacing R_s in (2) with $\hat{R}_s$ in (19), the estimator of $\alpha\beta$-axes currents can be constructed from following equation,

$$\begin{cases}\dfrac{\mathrm{d}\hat{i}_\alpha}{\mathrm{d}t}=\dfrac{1}{L}(u_\alpha-\hat{R}_s\hat{i}_\alpha+\mathrm{p}\omega_r\psi_\mathrm{m}\sin\theta)\\ \dfrac{\mathrm{d}\hat{i}_\beta}{\mathrm{d}t}=\dfrac{1}{L}(u_\beta-\hat{R}_s\hat{i}_\beta-\mathrm{p}\omega_r\psi_\mathrm{m}\cos\theta)\end{cases} \tag{20}$$

By combining (8), (19) and (20), the block diagram of the designed adaptive observer is established as shown in Figure 2, which treats the stator voltages, rotor electrical position and speed as the inputs, the *dq*-axes currents and stator resistance as outputs when only phase-*b* current is measured.

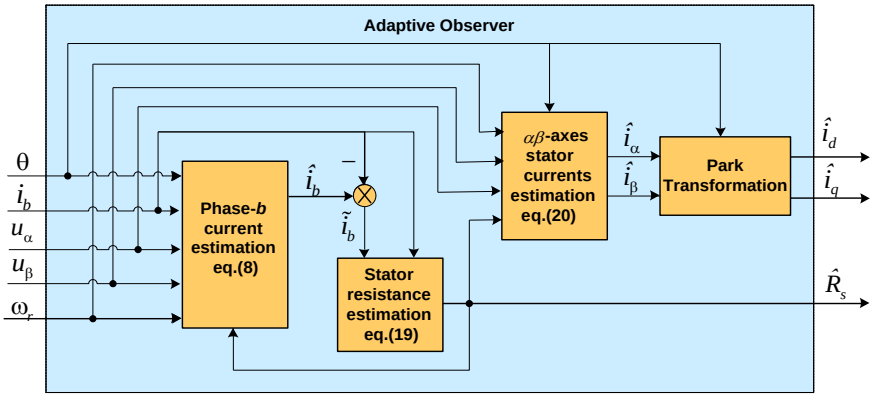

Figure 2. Block Diagram of the Proposed Adaptive Observer

Remark 1. From Figure 2, it can be seen that estimating the phase-*b* current is a key step in construction of the adaptive observer and also a primary premise. The error between the phase-*b* measured current and its estimated value must be guaranteed to converge towards zero.

Remark 2. From (8) and (19), it can be seen that although the coupling relationship exists between $\hat{i}_b$ and $\hat{R}_s$, the design process does not need to calculate decouple of them. In fact, the phase-*b* current estimation equation (8) and the stator resistance adaptive law (19) are implemented and solved all together.

Remark 3. The convergence rate of the observer is dependent on the observer gains k_1 and k_2, which should be chosen to be large enough such that the observer responds as soon as possible.

Remark 4. The estimated *dq*-axes currents in Figure 2 will be applied to MPTC as shown in Figure 1.

Remark 5. From (5), the estimation of phase-*a* current in *abc*-frame is equal to that of α-axis current in $\alpha\beta$-frame as follows,

$$\hat{i}_a = \hat{i}_\alpha \tag{21}$$

Accordingly, the estimation of phase-*c* current in *abc*-frame can be obtained as follows,

$$\hat{i}_c = -\left(i_b + \hat{i}_\alpha\right)$$

3.2. Model Predictive Torque Control

The basic idea of MPTC is to predict the future behavior of the variables over a time frame based on the model of the system. In fact, MPTC is an extension of DTC, as it replaces the look-up table of DTC with an online optimization process in the control of machine torque and flux. Different from the employments of hysteresis comparators and switching table in conventional DTC, the principle of vector selection in MPTC is based on evaluating a defined cost function. The selected voltage vector from conventional switching table in DTC is not necessarily the best one in terms of reducing torque and flux ripples. There are limited discrete voltage vectors in the two-level inverter-fed PMSM drives. As a result, it is possible to evaluate the effect of each voltage vector and select the one minimizing the cost function.

As shown in Figure.1, MPTC includes three parts: cost function minimization, predictive model and flux & torque estimators.

3.2.1. Cost Function Minimization

For MPTC, the cost function is such chosen that both torque and flux at the end of the cycle is as close as possible to the reference value. Generally, the minimum value of cost function is defined as

$$\begin{aligned} &\min.g = \left|T_e^* - T_e^{k+1}\right| + k_3\left\|\psi_s^*\right| - \left|\psi_s^{k+1}\right\| \\ &s.t. \quad u_s^k \in \{V_1,\ V_2,\ \cdots\ V_5,\ V_6\} \end{aligned} \tag{22}$$

where T_e^* and ψ_s^* are reference values for torque and stator flux, respectively. T_e^{k+1} and ψ_s^{k+1} predictions for torque and stator flux at $(k+1)$th instant, respectively. V_1, V_2, V_3, V_4, V_5, and V_6 are six nonzero voltage space vectors and can be generated by three phase VSI with respect to the different switches states. A set of voltage space vectors u_s^k at kth instant is defined as

$$u_s^k = 2V_{dc}\left[S_a^k + e^{i2\pi/3}S_b^k + \left(e^{i2\pi/3}\right)^2 S_c^k\right]/3 \tag{23}$$

where S_x^k (x=a,b,c) at kth instant is upper power switch state of one of three legs . S_x^k =1 or S_x^k =0 when upper power switch of one leg is on or off. k_3 is the weighting factor. The selection of k_3 is still an open problem for answer [36].

3.2.2. Predictive Model for Stator Currents

According to (1), the prediction of the stator current at the next sampling instant is expressed as

$$\begin{cases} i_d^{k+1} = i_d^k + \dfrac{1}{L}(-R_s i_d^k + \mathrm{p}\omega_r^k L i_q^k + u_d^k)T_s \\ i_q^{k+1} = i_q^k + \dfrac{1}{L}(-R_s i_q^k - \mathrm{p}\omega_r^k L i_d^k - \mathrm{p}\omega_r^k \psi_m + u_q^k)T_s \end{cases} \tag{24}$$

where i_d^k, i_q^k and R_s are replaced by the corresponding estimated values coming from the observer in Fig.2. T_s is the sampling period.

3.2.3. Torque & Flux Estimators

In *dq*-frame, the current-based flux-linkage ψ_d and ψ_q can be expressed as following vector [29]

$$\begin{bmatrix} \psi_d^{k+1} \\ \psi_q^{k+1} \end{bmatrix} = \begin{bmatrix} L & 0 \\ 0 & L \end{bmatrix} \begin{bmatrix} i_d^{k+1} \\ i_q^{k+1} \end{bmatrix} + \begin{bmatrix} \psi_m \\ 0 \end{bmatrix} \tag{25}$$

The magnitude of stator flux linkage ψ_s is

$$\psi_s^{k+1} = \sqrt{\left(\psi_d^{k+1}\right)^2 + \left(\psi_q^{k+1}\right)^2} \tag{26}$$

Electromagnetic torque developed in *dq*- frame can be estimated as following

$$T_e^{k+1} = \frac{3}{2} p \psi_m i_q^{k+1} \tag{27}$$

Substituting (24) into (27), the torque is estimated.

3.2.4. Stability Analysis of MPTC for PMSM Drive System

PMSM drive system with the MPTC design can be proved to be globally asymptotically stable. The detailed proof is omitted here due to space limitations. The interested reader is referred to [37].

3.3. Maximum Torque per Ampere

According to the principle of maximum torque per ampere, the reference stator flux linkage ψ_s^* can be calculated as follows

$$\psi_s^* = \sqrt{\left(T_e^* L \Big/ \frac{3}{2} p \psi_m\right)^2 + \left(i_d^* L + \psi_m\right)^2} \tag{28}$$

where i_d^* is reference value of *d*-axis current and assumed to be zero, *i.e.*, $i_d^* = 0$

As a result, the corresponding reference stator flux linkage ψ_s^* is rewritten as

$$\psi_s^* = \sqrt{\left(T_e^* L \Big/ \frac{3}{2} p \psi_m\right)^2 + \psi_m^2} \tag{29}$$

3.4. Power Unit and PI Controller

The power unit adopts 2-level 3-phase VSI. PI controller is used to regulate the rotor speed [32], and its parameters are determined by differential evolution algorithm [38]-[39].

4. Simulation Result and Analysis

In order to validate the effective of proposed control scheme, the designed control system from Figure 1 is implemented in Matlab/Simulink/Simscape platform. The parameters of PMSM are given in Table 1. In order to verify estimation accuracy of the observer and control performance of the single phase current sensor-based MPTC drive system, two scenarios of numerical simulation are provided and compared, which correspond to MPTC with two phase current sensors (phase-*a* and -*b* sensors) and MPTC with single phase current sensor (phase-*b*), respectively. For convenience sake, the former scenario is marked as Case one and the latter one as Case two.

Table 1. Parameters of PMSM

Symbol	Quantity	Value
R_s	Nominal phase resistance	2.875Ω
L_d , L_q	*dq*-coordinate inductance	0.0085H
ψ_{m}	Rotor magnetic flux	0.175Wb
p	Number of pole pairs	4
V_{dc}	DC bus voltage	300V
n_N	Rated speed	2000rpm
T_n	Rated torque	4Nm
J	Moment of inertia	0.0008Kg.m^2
B_{m}	Viscous friction coefficient	0.001Nms
T_{f}	Coulomb friction torque	0

The sampling period is 10μs, and value k_3 is selected to be 200. The parameters of PI in MPTC for two scenarios are selected as follows,

$K_p = 0.6, K_I = 0.2$

As for the observer, the parameters of PI in stator resistance estimation (19) are

$K_{P(R_s)} = 0.001, K_{I(R_s)} = 2$

And other parameters of the observer are respectively selected as

$k_1 = 30, k_2 = 5000, r = 1000$

The following first presents the simulation comparison results of the above-mentioned two scenarios. Thereafter, the simulation results corresponding to three operating conditions are presented, respectively.

4.1. Performance Comparison of Two Scenarios

Figure 3 shows their comparison results in terms of stator currents, stator resistance, rotor speed and torque when the reference speed n^* is set to 1000 rpm, the load torque of 4Nm. From Figure 3(a)-3(e), it can be seen that, for adaptive observer of Case two, its estimated *a*-axis and *c*-axis currents in *abc*-frame and *d*-axis and *q*-axis currents in *dq*-frame rapidly track corresponding ones of Case one, and its estimated stator resistance converges to the nominal value accurately. Figure 3(f)-3(g) show that, for MPTC system of Case two, its speed and torque can be regulated in a satisfactory manner and has almost as good performance as MPTC system of Case one.

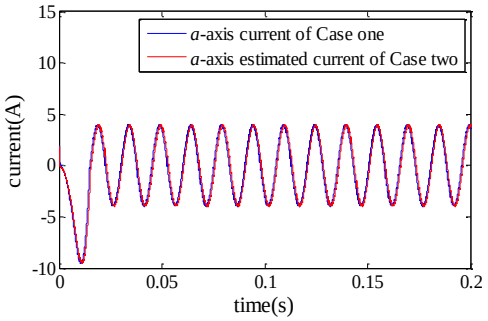

(a) *a*-axis Stator Current in *abc*-frame

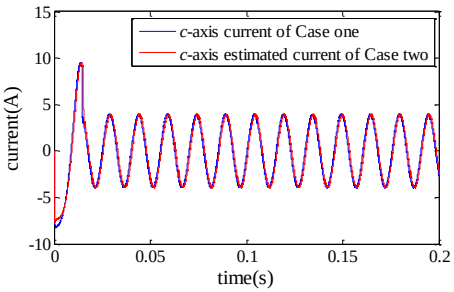

(b) *c*-axis Stator Current in *abc*-frame

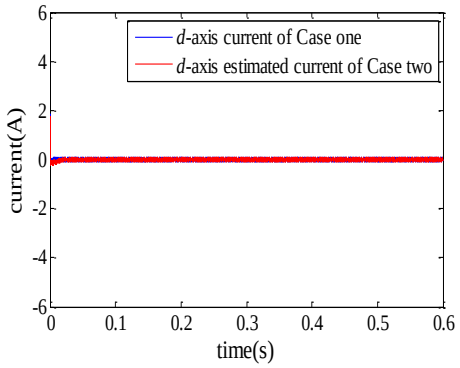

(c) d-axis Stator Current in dq-frame

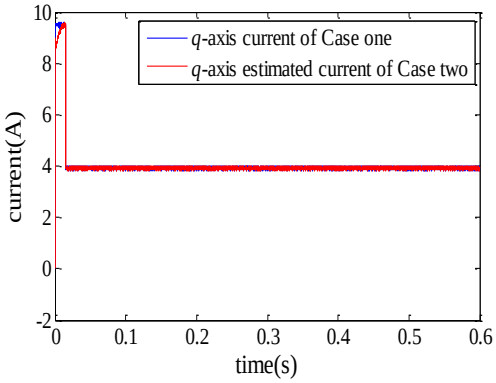

(d) q-axis Stator Current in dq-frame

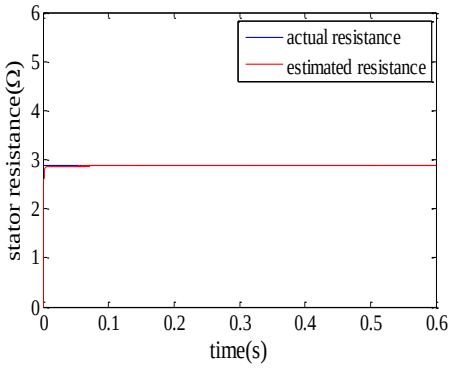

(e) Actual and Estimated Stator Resistance

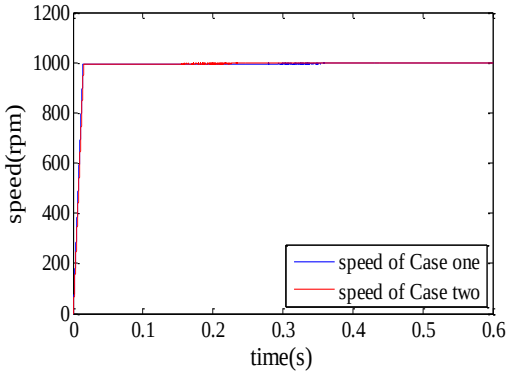

(f) Rotor Speed Response

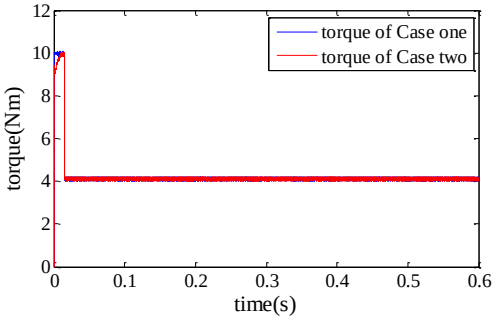

(g) Torque response

Figure 3. Dynamic Response Comparison between Case One and Case Two

4.2. Performance Comparison under the Variation of Stator Resistance

Here, the stator resistance is changed from its nominal value 2.875Ω to 5Ω at 0.3 seconds. Figure 4 shows the comparison of two scenarios. From Figure 4(a)-4(e), it can be observed seen that, for adaptive observer of Case two, its estimated resistance value can rapidly follow actual resistance change, and their estimated *a*-axis and *c*-axis currents in *abc*-frame and *d*-axis and *q*-axis currents in *dq*-frame rapidly track corresponding ones of Case one. Figure 4(f)-4(g) show that for MPTC system of Case two, its ability against resistance variation is no less strong than Case one's.

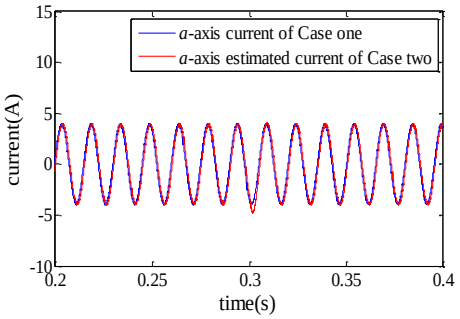

(a) a-axis Stator Current in abc-frame

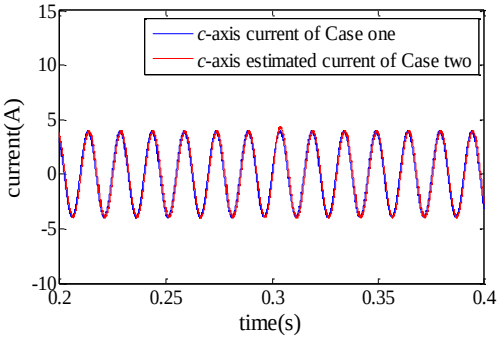

(b) c-axis Stator Current in abc-frame

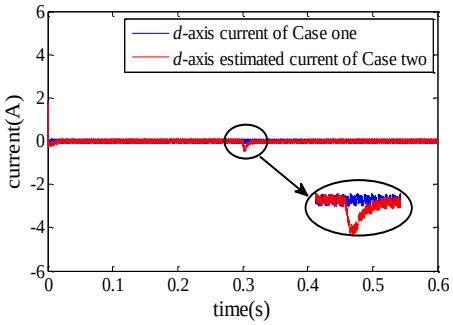

(c) d-axis Stator Current in dq-frame

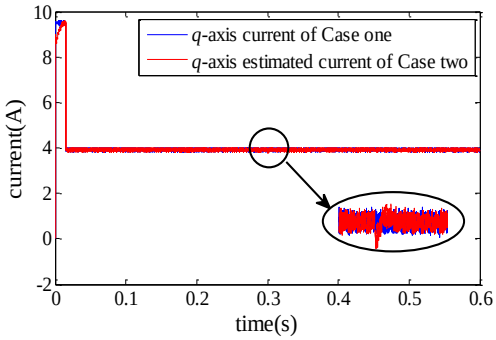

(d) q-axis Stator Current in dq-frame

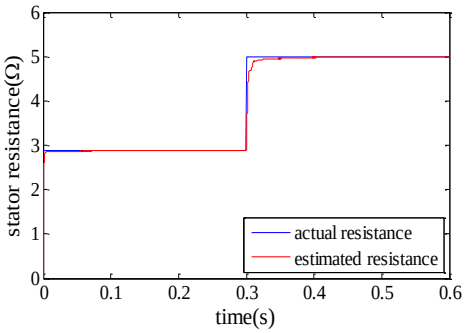

(e) Actual and Estimated Stator Resistance

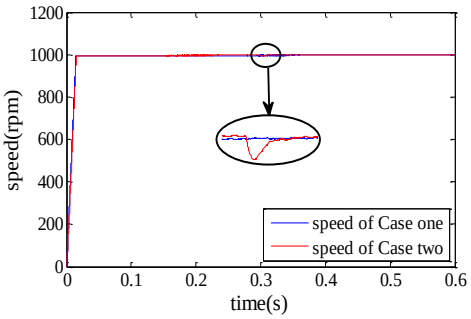

(f) Rotor Speed Response

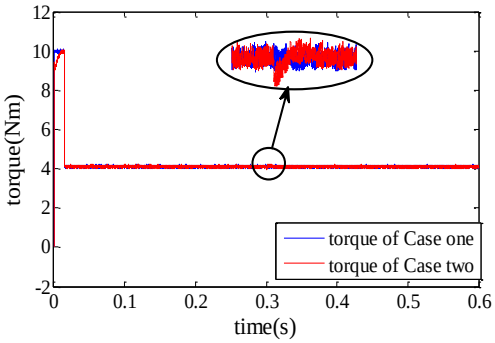

(g) Torque Response

Figure 4. Dynamic Response Comparison between Case one and Case Two under the Variation of Stator Resistance

4.3. Performance Comparison under the Variation of Stator Resistance

Here, the load torque of 4Nm is decreased to 1 Nm at 0.2 seconds and the stator resistance is changed from its nominal value 2.875Ω to 5Ω at 0.3 seconds. Figure 5 shows the comparison of two scenarios. From Figure 5(a)-5(e), it can be seen that, for adaptive observer of Case two, its estimated *a*-axis and *c*-axis currents in *abc*-frame and *d*-axis and *q*-axis currents in *dq*-frame rapidly track corresponding ones of Case one, and its estimated stator resistance converges to the nominal value accurately. Figure 5(f)-5(g) show that for MPTC system of Case two, the speed and torque can sharply adapt to the change of external load in a satisfactory manner, and its capable of accommodating the challenge of load disturbance is not inferior to Case one's.

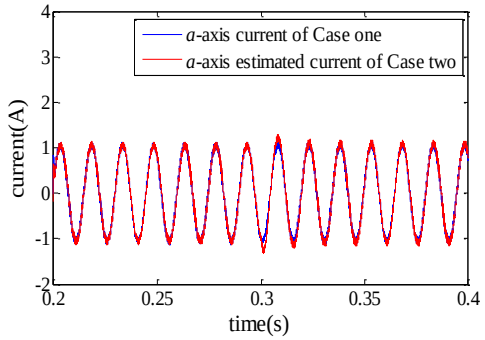

(a) *a*-axis Stator Current in *abc*-frame

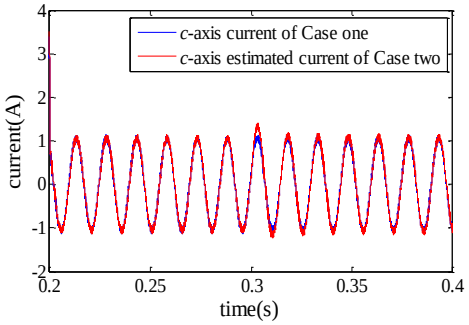

(b) *c*-axis Stator Current in *abc*-frame

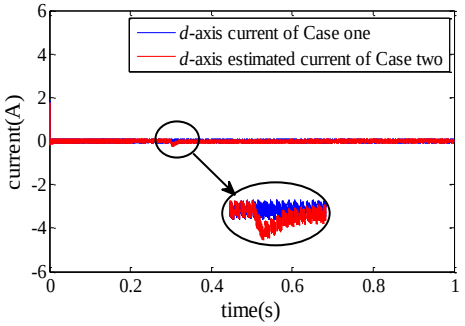

(c) d-axis Stator Current in dq-frame

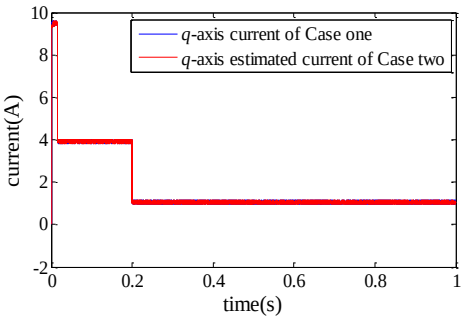

(d) q-axis Stator Current in dq-frame

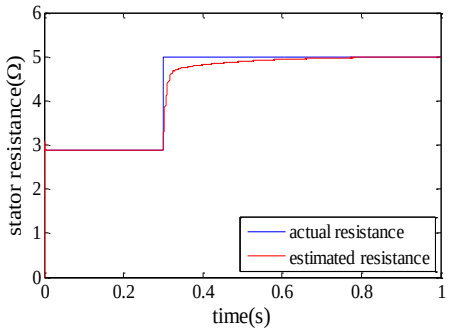

(e) Actual and Estimated Stator Resistance

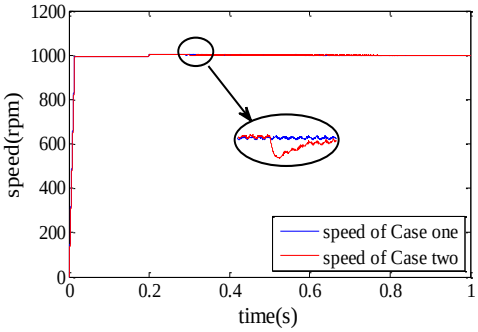

(f) Rotor Speed Response

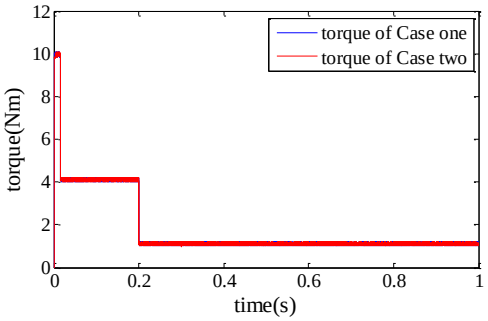

(g) Torque Response

Figure 5. Dynamic Response Comparison between Case One and Case Two under the Variation of Load Torque

4.4. Performance Comparison under the Variation of Reference Speed

Here, reference speed n^* of 1000 rpm is decreased to 600 rpm at 0.2 seconds and the stator resistance is changed from its nominal value 2.875Ω to 5Ω at 0.3 seconds. Figure 6 shows the comparison of two scenarios. From Figure 6(a)-6(e), it can be seen that, for adaptive observer of Case two, its estimated *a*-axis and *c*-axis currents in *abc*-frame and *d*-axis and *q*-axis currents in *dq*-frame rapidly track corresponding ones of Case one, and its estimated stator resistance converges to the nominal value accurately. From Figure 6(f)-6(g), it can be seen that for MPTC system of Case two, although a sharp pulse of torque arises at the step speed change, torque is rapidly regulated to its reference and the accuracy of speed tracking is high. Hence Case two's ability to deal with speed change is not worse than Case one's.

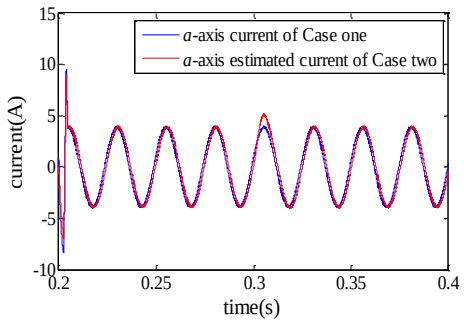

(a) a-axis Stator Current in abc-frame

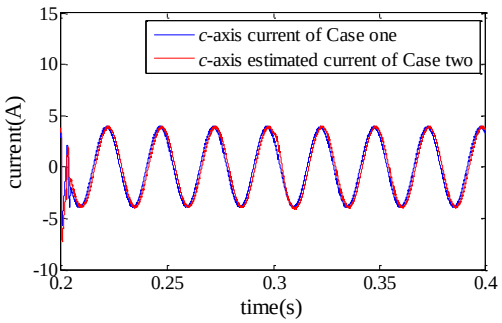

(b) c-axis Stator Current in abc-frame

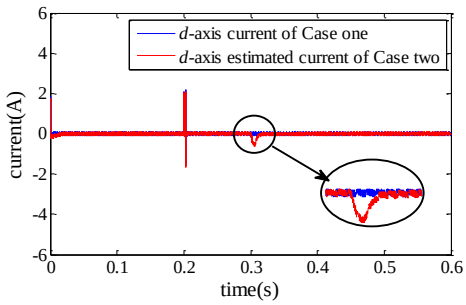

(c) d-axis Stator Current in dq-frame

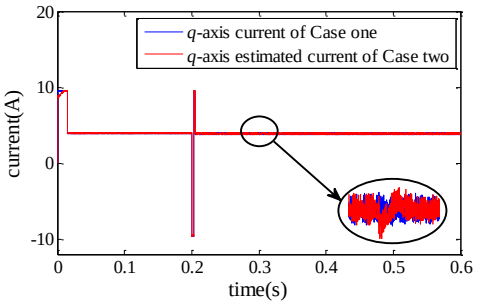

(d) q-axis Stator Current in dq-frame

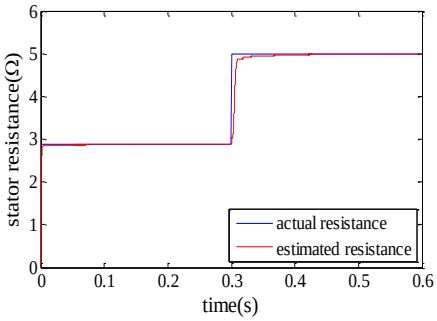

(e) Actual and Estimated Stator Resistance

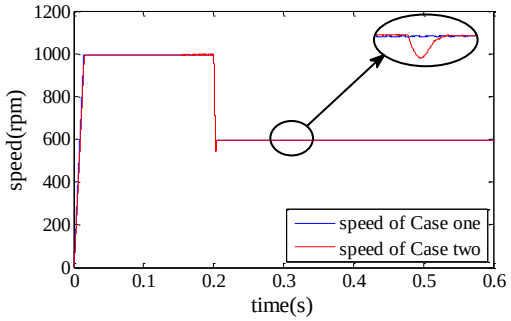

(f) Rotor Speed Response

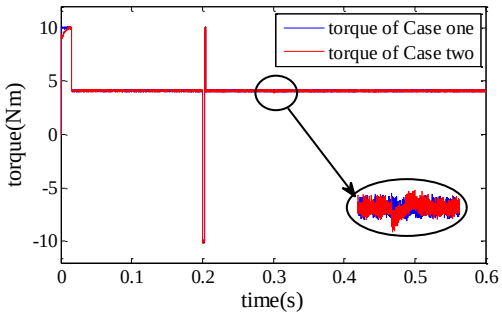

(g) TorqueResponse

Figure 6. Dynamic Response Comparison between Case One and Case Two under the Variation of Speed

5. Conclusion

This paper puts forward a novel adaptive observer-based MPTC scheme for three-phase PMSM drive system with only one phase current sensor. The designed adaptive observer is capable of concurrent online estimation of stator currents and stator resistance under the assumption that rotor speed and position are available for measurement. Stability and convergence of the observer are analytically verified based on Lyapunov stability theory. MPTC strategy is employed to reduce the torque & flux ripples and improve performance. The proposed observer can be embedded into a fault resilient PMSM drive system. In case of a phase current sensor failure, the proposed observer can be used as a virtual sensor. The designed single phase current sensor-based MPTC can guarantee that PMSM drives system achieves satisfactory torque and speed control and improve strong robustness. Comprehensive simulation validates the feasibility and effectiveness of the proposed scheme.

Acknowledgements

This work was supported by National Natural Science Foundation of China (No.61463025).

References

[1] D. Chung and S. Sul, "Analysis and compensation of current measurement error in vector-controlled AC motor drives", IEEE Trans. on Industrial Application, vol. 34, no. 2, **(1998)**, pp.340–345.
[2] Y. S. Jeong, S. K. Sul, E. Schulz and N. R. Patel, "Fault Detection and Fault-Tolerant Control of Interior Permanent-Magnet Motor Drive System for Electric Vehicle", IEEE Trans. on Industrial Application, vol. 41, no. 1, **(2005)**, pp.46-51.
[3] J. T. Boys, "Novel current sensor for PWM ac drives", IEE Proceedings B: Electric Power Applications, vol. 135, **(1988)**, pp.27-32.
[4] H. Y. Ma, K. Sun, Q. Wei and L. P. Huang, "Phase current reconstruction for AC motor adjustable speed drives in the over modulation method", Journal of Tsinghua University, vol.50, no.11, **(2010)**, pp.1757-1761.
[5] T. C. Green and B. W. Williams, "Derivation of motor line-current waveforms from the DC-link current of an inverter", IEE Proceedings B: Electric Power Applications, vol.136, no.4, **(1989)**, pp.196-204.
[6] H. Kim and T. M. Jahns, "Phase Current Reconstruction for AC Motor Drives Using a DC Link Single Current Sensor and Measurement Voltage Vectors", IEEE Transaction on Power Electronics, vol.21, no.5, **(2006)**, pp.1413-1419.
[7] J. Ha, "Voltage Injection Method for Three Phase Current Reconstruction in PWM Inverters Using a Single Sensor", IEEE Transaction on Power Electronics, vol.24, no.3, **(2009)**, pp.767-775.
[8] J. Ha, "Current Prediction in Vector Controlled PWM Inverters Using Single DC-Link Current Sensor", IEEE Trans. on Industrial Electronics, vol.57, no.2, **(2010)**, pp.716-726.
[9] K. Sun, Q. Wei, L. P. Huang and K. Matsuse, "An Over modulation Method for PWM Inverter Fed IPMSM Drive with Single Current Sensor", IEEE Transaction on Industrial Electronics, vol.57, no.10, **(2010)**, pp.3395-3404.
[10] Y. K. Gu, F. L. Ni, D. P Yang and H. Liu, "Switching State Phase Shift Method for Three Phase Current Reconstruction with a Single DC-Link Current Sensor", IEEE Transaction on Industrial Electronics, vol.58, no.11, **(2011)**, pp.5186-5194.
[11] B. Metidji, N. Taib, L. Baghli, T. Rekioua and S. Bacha, "Low Cost Direct Torque Control Algorithm for Induction Motor without AC Phase Current Sensors", IEEE Transaction on Power Electronics, vol.27, no.9, **(2012)**, pp.4132-4139.
[12] Y. S. Lai, Y. K. Lin and C. W. Chen, "New Hybrid Pulse width Modulation Technique to Reduce Current Distortion and Extend Current Reconstruction Range for a Three-Phase Inverter Using Only DC-link Sensor", IEEE Transaction on Power Electronics, vol.28, no.3, **(2013)**, pp.1331-1337.
[13] H. F. Lu, X. M. Cheng, W. L. Qu, S. Sheng, Y. T. Li and Z.Y. Wang, "A Three-Phase Current Reconstruction Technique Using Single DC Current Sensor Based on TSPWM", IEEE Transaction on Power Electronics, vol.29, no.3, **(2014)**, pp.1542-1550.
[14] Y. Gu, F. Ni, D. Yang, J. Dang and H. Liu, "Novel method for phase current reconstruction using a single dc-link current sensor", Electric machine and control, vol.13, no.6, **(2009)**, pp.811-816.
[15] M. Carpaneto, P. Fazio, M. Marchesoni and G. Parodi, "Dynamic Performance Evaluation of Sensorless Permanent-Magnet synchronous Motor Drives With Reduced Current Sensors", IEEE Transaction on Industrial Electronics, vol.59, no.12, **(2012)**, pp.4579-4589.
[16] H. F. Lu, X. M. Cheng, W. L. Qu, S. Sheng, Y. T. Li and Z. Y. Wang, "A Three-Phase Current Reconstruction Technique Using Single DC Current Sensor Based on TSPWM", IEEE Transaction on Power Electronics, vol.29, no.3, **(2014)**, pp.1542-1550.
[17] Y. H. Cho, T. LaBella and J. Lai, "A Three-Phase Current Reconstruction Strategy With Online Current Offset Compensation Using a Single Current Sensor", IEEE Transaction on Industrial Electronics, vol.59, no.7, **(2012)**, pp.2924-2933.
[18] V. Verma, C. Chakraborty, S. Maiti and Y. Hori, "Speed Sensorless Vector Controlled Induction Motor Drive Using Single Current Sensor", IEEE Transaction on Energy Conversion, vol.28, no.4, **(2013)**, pp.938-950.
[19] Y. Da, X. Shi and M. Krishnamurthy, "A Novel Universal Sensor Concept for Survivable PMSM Drives", IEEE Transaction on Power Electronics, vol.28, no.12, **(2013)**, pp.5630-5638.
[20] F. R. Salmasi and T. A. Najafabadi, "An Adaptive Observer with Online Rotor and Stator Resistance Estimation for Induction Motors with One Phase Current Sensor", IEEE Transaction on Energy Conversion, vol.26, no.3, **(2011)**, pp.959-966.
[21] Q. F. Teng, J. Y. Bai, J. G. Zhu and Y. G. Guo, "Current sensorless model predictive torque control based on adaptive backstepping observer for PMSM drives", WSEAS Transactions on systems, vol.13, **(2014)**, pp.187-202.
[22] Q. F. Teng, J. G. Zhu, T. S. Wang and G. Lei, "Fault Tolerant Direct Torque Control for Three Phase Permanent Magnet Synchronous Motors", WSEAS Transactions on systems, vol.11, no.8, **(2012)**, pp.465-476.
[23] S. Kouro, P. Cortes, R. Vargas, U. Ammann and J. Rocriguez, "Model Predictive Control—A Simple and Powerful Method to Control Power Converters", IEEE Transaction on Industrial Electronics, vol.56, no.6, **(2009)**, pp.1826-1838.

[24] H. Miranda, P. Cortes, J. I. Yuz and J. Rodriguez, "Predictive torque control of induction machines based on state-space models", IEEE Transaction on Industry Electronics, vol.56, no.6, **(2009)**, pp.1916-1924.
[25] M. Preindl and S. Bolognani, "Model Predictive Direct Torque Control with Finite Control Set for PMSM Drive Systems, Part 2: Field Weakening Operation", IEEE Transaction on Industrial Informatics, vol.9, no.2, **(2013)**, pp.648-657.
[26] R. P. Aguilera, P. Lezana and D. E. Quevedo, "Finite-Control-Set Model Predictive Control With Improved Steady-State Performance", IEEE Transaction on Industrial Informatics, vol.9, no.2, **(2013)**, pp. 658-667.
[27] T. Geyer, "Model Predictive Direct Current Control: Formulation of the Stator Current Bounds and the Concept of the Switching Horizon", IEEE Transaction on Industrial Application, vol.18, no. 2, **(2012)**, pp.47-59.
[28] T. Geyer, "A Comparison of Control and Modulation Schemes for Medium-Voltage Drives: Emerging Predictive Control Concepts Versus PWM-Based Schemes", IEEE Transaction on Industrial Application, vol.47, no.3, **(2011)**, pp.1380-1389.
[29] T. Geyer, "Model Predictive Direct Torque Control—Part Ⅰ: Concept, Algorithm, and Analysis", IEEE Transaction on Industrial Electronics, vol.56, no.6, **(2009)**, pp.1894-1905.
[30] M. Preindl and S. Bolognani, "Model Predictive Direct Speed Control with Finite Control Set of PMSM Drive Systems", IEEE Transaction on Power Electronics, vol.28, no.2, **(2013)**, pp.1007-1015.
[31] S. Chai, L. Wang and E. Rogers, "A Cascade MPC Control Structure for a PMSM with Speed Ripple Minimization", IEEE Transaction on Industrial Electronics, vol.60, no.8, **(2013)**, pp.2978-2987.
[32] Q. F. Teng, J. Y. Bai, J. G. Zhu and Y. X. Sun, "Fault Tolerant Model Predictive Control of Three-Phase Permanent Magnet Synchronous Motors", WSEAS Transactions on systems, vol.8, no.12, **(2013)**, pp.385-397.
[33] Q. F. Teng, J. Y. Bai, J. G. Zhu and Y. G. Guo, "Sensorless model predictive torque control using sliding-mode model reference adaptive system observer for permanent magnet synchronous motor drive systems", Control Theory & Applications, vol.32, no. 2, **(2015)**, pp.150-161.
[34] C. E. Garcia, D. M. Prett and M. Morari, "Model predictive control: Theory and practice—A survey", Automatica, vol.25, no.3, **(1989)**, pp.335-348.
[35] Y. C. Zhang, J. G. Zhu and W. Xu, "Predictive torque control of permanent magnet synchronous motor drive with reduced switching frequency", Proceedings of 2010 International Conference on Electrical Machines and Systems, Incheon, South Korea, **(2010)** October 10-13.
[36] T. Geyer, "Generalized model predictive direct torque control: Long prediction horizons and minimization of switching losses", Proceedings of 48th IEEE Conference on Decision and Control, Shanghai, China, **(2009)** December 16-18.
[37] S. K. Kim, J. S. Kim and Y. I. Lee, "Model Predictive Control (MPC) based Direct Torque Control (DTC) of Permanent Magnet Synchronous Motors (PMSMs)", Proceedings of 22nd IEEE International Symposium on Industrial Electronics, Taipei, Taiwan, **(2013)**.
[38] R. Oonsivilai and A. Oonsivilai, "Differential Evolution Application in Temperature Profile of Fermenting Process", WSEAS Transactions on Systems, vol. 9, no. 6, **(2010)**, pp.618-628.
[39] Ahuja and A. Sanjeev Kumar, "Design of fractional order pid controller for DC motor using evolutionary optimization techniques", WSEAS Transactions on Systems and Control, vol. 9, **(2014)**, pp.171-182.

Authors

QingFang Teng, she received the B.S. degree in aviation automatic control from Northwestern Polytechnical University, Xi'an, Shangxi, in 1985, the M.S. degree and the Ph.D. degree in traffic information engineering and control from Lanzhou Jiaotong University, Gansu Province, China, in 2003 and 2008. She is currently Professor of Control Engineering at Department of Automatical & Electrical Engineering, Lanzhou Jiaotong University. Her research interests include control theory and engineering, electrical machine control.

